

PACS numbers: 42.55.Rz; 42.65.Re; 41.60.Cr
DOI: 10.1070/QE2007v037n08ABEH013564

Development of a yearlong maintenance-free terawatt Ti : Sapphire laser system with a 3D UV-pulse shaping system for THG

H. Tomizawa, H. Dewa, H. Hanaki, F. Matsui

***Abstract*. Laser sources that feature a controlled pulse shape and long-term stability are required in a wide range of scientific fields. We developed a maintenance-free 3D-shaped UV-laser system for the photoinjector (RF gun photocathode) of an X-ray SASE free electron laser (FEL). The laser pulse-energy stability was improved to 0.2 % – 0.3 % (rms, 10 pps, 0.4 TW in femtosecond operation) at the fundamental wavelength and to 0.7 % – 1.4 % at the third-harmonic wavelength. This stability was continuously maintained for five months, 24 hours a day. Such improvement reflects an ability to stabilise the laser system in a humidity-controlled clean room. The pulse-energy stability of a mode-locked femtosecond oscillator was continuously held at 0.3 % (p – p) for five months, 24 hours a day. In addition, the ideal spatial and temporal profiles of a shot-by-shot single UV-laser pulse are essential to suppress the emittance of the electron-beam pulse generated by the photocathode of the RF gun. We apply a deformable mirror that automatically shapes the spatial UV-laser profile with a feedback routine, based on a genetic algorithm, and a pulse stacker for temporal shaping at the same time. The 3D shape of the laser pulse is spatially top-hat (flattop) and temporally – a square stacked pulse. We apply the *Q*-scan method to evaluate the emittance of the electron beam generated by a 3D-shaped laser pulse. By using a 3D-shaped laser pulse of diameter 0.8 mm on the cathode and duration 10 ps (FWHM), we obtain a minimum horizontal normalised emittance of 1.4π mm mrad with beam energy of 26 MeV, holding its net charge to a 0.4 nC pulse^{-1}. At a higher net charge of 1.0 nC pulse^{-1}, the minimum beam emittance is 2.3π mm mrad with equivalent diameter and a longer pulse duration of 20 ps (FWHM). In this study, we demonstrate 3D shaping [both temporal (1D) and spatial (2D)] short pulse (5 – 20 ps) laser beam as an ideal light source for yearlong stable generation of a low emittance electron beam with a high charge (1 – 2 nC pulse^{-1}). Here, we report the principle and development process of our beam-quality control systems.**

H. Tomizawa, H. Dewa, H. Hanaki Accelerator Division, Japan Synchrotron Radiation Research Institute (SPring-8) Kouto, Mikazuki-cho, Sayo-gun, Hyogo 679-5198, Japan;
F. Matsui Creative & Advanced Research Department, Industrial Technology Center of Fukui Prefecture 61, Kawaiwashitsuka-cho, Fukui City 910-0102, Japan

Received 12 March 2007
Kvantovaya Elektronika **37** (8) 697 – 705 (2007)
Submitted in English

Keywords: *beam quality control, Ti : Sapphire laser, terawatt femtosecond laser, maintenance-free laser system, long-term continuous stable operation, spatial shaping, pulse shaping, 3D laser pulse shaping, adaptive optics, deformable mirror (DM), genetic algorithm, spatial light modulator (SLM), simulated annealing algorithms, photoinjector, X-ray light sources, free electron laser (FEL), energy recovery Linac (ERL), RF gun photocathode.*

1. Introduction

We have been developing a stable and highly efficient pulsed UV laser source for a RF gun photocathode [1] that in turn produces a high-brightness electron beam for future X-ray light sources [free electron laser (FEL), Compton back scattering, etc.] since 1996 at SPring-8 (Synchrotron Radiation Research Group). The electron source for several X-ray FEL projects [2 – 4] requires a very-low-emittance (high-brightness) electron beam as low as 1π mm mrad. The most reliable candidate for this high-brightness electron source is a RF gun photocathode. This type of gun generates an electron beam pulse from a photocathode illuminated by a laser pulse. Our development of this gun is oriented toward a yearlong stable system for user experiments. It is necessary for the copper cathode of this RF gun to have a UV-laser pulse with a pulse width of $\tau_p \sim 10$ ps and a photon energy of ~ 4 eV. Since we started to develop the laser test facility, two issues related to the laser light source have arisen. One is the energy stability of the UV-laser light source (see Section 2). Therefore, we have stabilised the third-harmonic generation (THG) of a CPA (chirped pulse amplification) Ti : Sapphire terawatt laser system (Fig. 1)* as the laser light source for the SPring-8 RF gun.

The other problem concerns the spatial and temporal laser profiles (see Section 3). To minimise the beam emittance of a RF gun photocathode, the laser pulse shape should be optimised three-dimensionally. Over the past five years at SPring-8's test facility for the photocathode laser light source, several 3D shaping systems have been developed from combinations of spatial (transverse: x, y axes) and temporal (longitudinal: z axis) pulse shaping methods (Fig.1). The spatial profile has to be modified with a microlens array [5] or a deformable mirror (DM) [6]. In addition, the temporal profile has to be modified with a spatial light modulator (SLM) [6, 7] or the pulse stacker described in this paper. One of the candidates for a reliable

* Colour images of all the Figures in the paper are available at http://www.turpion.org/suppl/qe/13564/tomizawa.pdf.

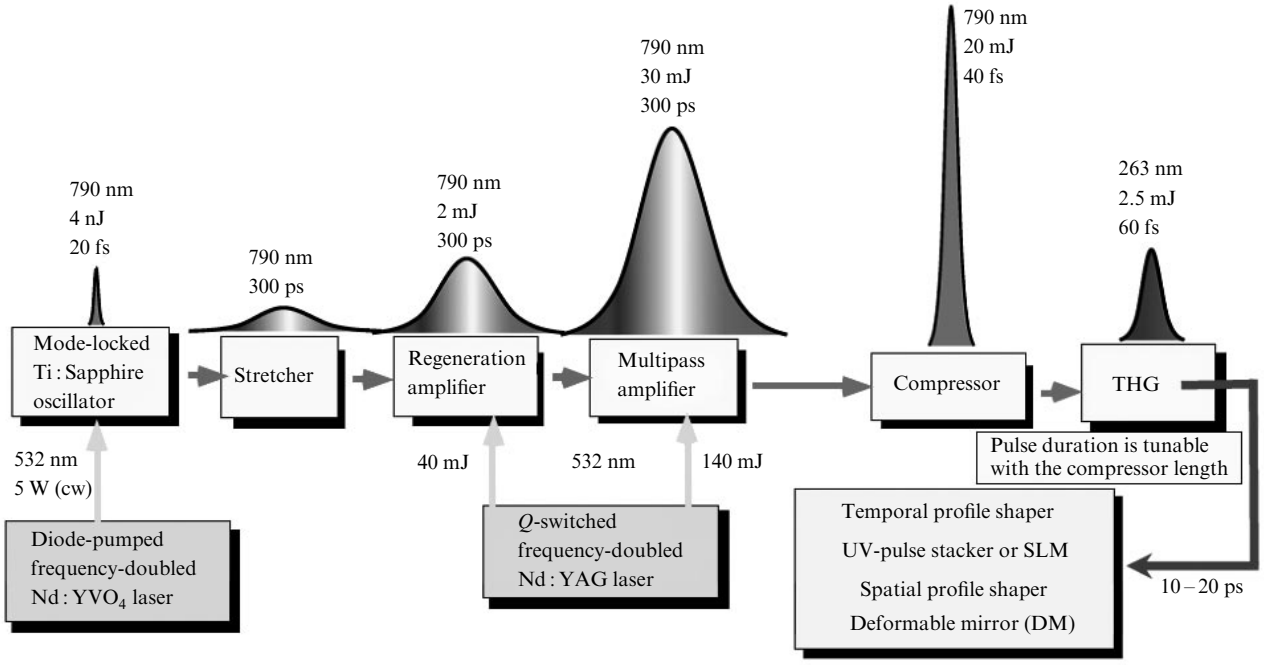

Figure 1. Laser pulse growth and three-dimensionally [spatially (2D) and temporally (1D)] shaping process. The pulse duration of THG (263 nm) depends on the compressor length at fundamental wavelength (790 nm). To obtain a 20-ps pulse by stacking eight micro pulses (three stages of pulse stackers), a 2.5-ps micro pulse should be initially prepared by shifting compressor length.

3D laser pulse shape has been the cylindrical shape (spatially top-hat and temporally square pulse). With a square-shaped 9-ps laser pulse, the lowest beam emittance of 1.2π mm mrad at 1.0 nC pulse^{-1} has already been achieved by J. Yang et al. [7]. Previously, we demonstrated a UV-laser spatial profile shaped as a quasi top-hat (flattop) with a deformable mirror used to automatically optimise it with a feedback routine based on a genetic algorithm. Using this top-hat laser pulse (diameter of 1.0 mm on the cathode) with a pulse duration of 5 ps (note: temporally, not square), we could obtain low-emittance beam generation of 1.7π mm mrad [6] at a net electron charge of 0.1 nC pulse^{-1}. However, the beam emittance at high charge was much larger because the charge density was too high. This indicates that a 5-ps laser pulse is too short for the laser spot diameter of 1 mm. Therefore, we prepared longer square laser pulses of 10 and 20 ps generated by stacking equivalently split 2.5-ps Gaussian pulses to obtain lower emittance in a higher-charge region. Three stages of pulse stacking can generate a 20-ps pulse from eight 2.5-ps micro pulses. The purpose of introducing longer laser pulses is to make the laser spot size on the cathode smaller while still decreasing the charge density. The small beam size helps to decrease the initial (thermal) emittance (at electron charge of zero), and the small charge density suppresses the space charge effect. Therefore, a long laser pulse is effective, especially in a high-charge region. A 3D particle tracking simulation predicted that smaller beam emittance could be obtained with a laser pulse length of about 20 ps at 1.0 nC pulse^{-1} [8]. This simulation result implies an important prediction, i.e. that electron pulse length can be maintained around 10 ps with both 10- and even 20-ps laser pulse lengths, due to electron pulse (bunch) length compression in the RF cavity.

2. Development of yearlong stable laser light source

We chose the third-harmonic generation (THG) of a CPA (chirped pulse amplification) Ti:Sapphire terawatt laser system (repetition rate of 10 Hz) as the laser light source for the SPring-8 RF gun. At THG (central wavelength: 263 nm), the femtosecond UV-laser pulse energy is up to 2.5 mJ pulse^{-1}. In its current form, the laser pulse energy stability has been improved to 0.2 % – 0.3 % (rms, 10 pps, 0.4 TW in femtosecond operation) at the fundamental and 0.7 % – 1.4 % at the third-harmonic generation. At the present state of development, this stability has been held for five months continuously, 24 hours a day (note that the flash lamp of the YAG laser pump source for the amplifiers has to be changed every two months). The improvements we had passively implemented were to stabilise the laser system as well as the environmental conditions. We introduced a humidity-control system that maintained humidity at 55 % [fluctuating by less than 2 % (p – p)] in a clean room to reduce electrostatic charge on the optics. This system keeps dust particles away from the optics and thus avoids burn-out damage. The temperature was kept constant at $21 \pm 0.3\,^{\circ}$C (p – p), monitored on the laser table. The improvement in THG stability results from the ability to stabilise the laser pump sources (*Q*-switched YAG) of the amplifiers with a temperature-controlled base plate in this humidity-controlled clean room. This base plate for YAG stabilisation maintained temperature at 25 °C [fluctuating by less than 0.1 % (p – p)]. In addition, we are testing a feedback system to control the long-term drift of the YAG laser due to the lifetime of the flash lamp, which is now limited to continuous operation of around five months (in our record, 119, 380, 846 shots at max.) while maintaining the high stability of the laser's pulse energy as mentioned above.

Aside from long-term drift of the pump YAG source, the long-term stability of the total laser system (in THG) depends only on the stability of mode-locking at the oscillator laser. A new oscillator laser (Femtosource Synergy; Femtolasers Produktions GmbH) was installed in our system in April 2005. This oscillator was passively stabilised with a temperature-controlled base plate [$21 \pm 0.1^{\circ}$C (p – p)]. In the first long-term continuous operation test run, its mode-locking was kept stable without any active stabilisation for one month (left figure of Fig. 2). However, laser parameters did not remain constant. This indicates that pointing of the pump laser or laser self-focusing in the crystal (due to change in the cavity length) causes a long-term drift (1 – 2 weeks). When the geometrical configuration of the laser cavity changes with these drifts, its mode-locking becomes unstable. Therefore, for the second test run, we introduced two active feedback systems (Femto-align and Femto-lock; Femtolasers Produktions GmbH) to lock the geometrical configuration of the laser cavity.

Femto-align is designed to compensate for long-term instabilities caused by environmental sources of interference such as thermal deformations or pump-pointing drift. Focusing on accuracy and security, it avoids mode-locking failures and reduces unexpected fluctuations. It monitors the output power and optimises operations whenever deviations occur. The active controlling mirror can compensate for long-term instabilities of the total laser system. On the other hand, Femto-lock is a sub-ps-jitter synchronisation for the oscillators. It allows locking the round-trip frequency of the oscillator pulses to a given reference RF-source (ROHDE & SCHWARZ GmbH & Co. KG: SMHU). The system comprises a fast piezo translator (PZT) in combination with a wide-range translation stage. This arrangement allows the unit to compensate for fast fluctuations ($\sim$ kHz) as well as for slow long-term drifts (e.g. mechanical deformations due to temperature drifts). This combination of feedback guarantees drift-free yearlong operation.

In the second long-term continuous operation test run, the oscillator was actively stabilised by utilising both Femto-align and Femto-lock, and it was operated at a locked repetition rate of 89.25 MHz. This long-term stability test had to be stopped for maintenance of the infrastructure. The pulse energy stability of the mode-locked femtosecond oscillator with a temperature-controlled base plate [$21 \pm 0.1\,^{\circ}$C (p – p)] was held at 0.3 % (p – p) for five months continuously, 24 hours a day (right figure of Fig. 2). Except for momentary line drop due to natural disasters (thunderbolts, etc.) or infrastructure maintenance, this oscillator has continuous yearlong operation while maintaining constant laser parameters (pulse energy, pulse duration, spectral distribution, etc.). The laser parameters are constant without any sign of instability. This indicates that the drifting deformations of the laser's geometrical configuration could have been locked within the stable region of mode-locking.

3. 3D shaping experiment with UV-laser pulse

The 3D UV-laser pulse shaping system combined with a deformable mirror (transverse: 2D) and pulse stacker (longitudinal: 1D) is shown in Fig. 3. Utilising the long-term stable UV-laser source described above, this system can generate a 3D cylindrical laser pulse. We explain both shaping techniques in the following sections.

3.1 Top-hat spatial profile optimisation with computer-aided deformable mirror

We used a computer-aided deformable mirror (top-right photo in Fig. 3) as a spatial shaper. This deformable mirror consists of an aluminium-coated, multilayer silicon nitride membrane and 59 small mirror actuators behind the reflective membrane with a center-to-center distance of 1.75 mm between the actuators. The outermost layer of the reflective membrane is protected with an MgF_2 coating to maintain reflectivity at about $\sim 80\,\%$ in the UV region. Adjusting voltages between the control electrodes on the boundary actuators results in fine adjustment of each mirror actuator; the adjustable region of the control

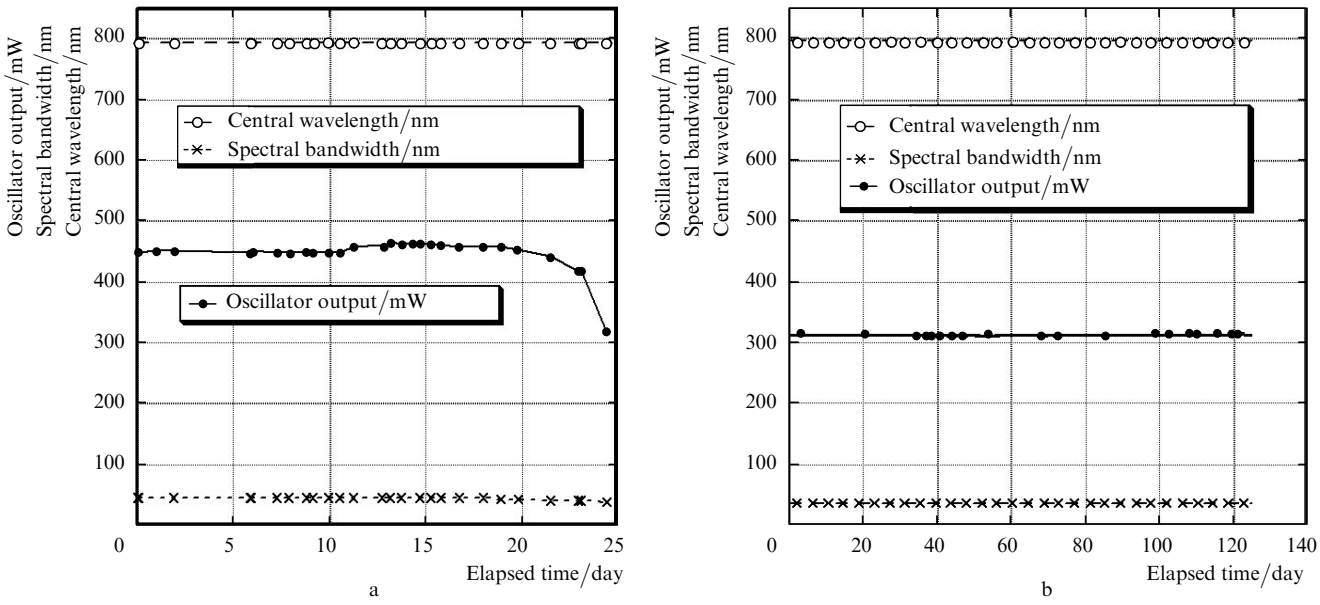

Figure 2. Improvement in laser oscillator's long-term stability [just passive (a), full-active (b), Femto-align & Femto-lock]. Full-active feed-backing, the mode-locking and spectral distribution have been kept constant.

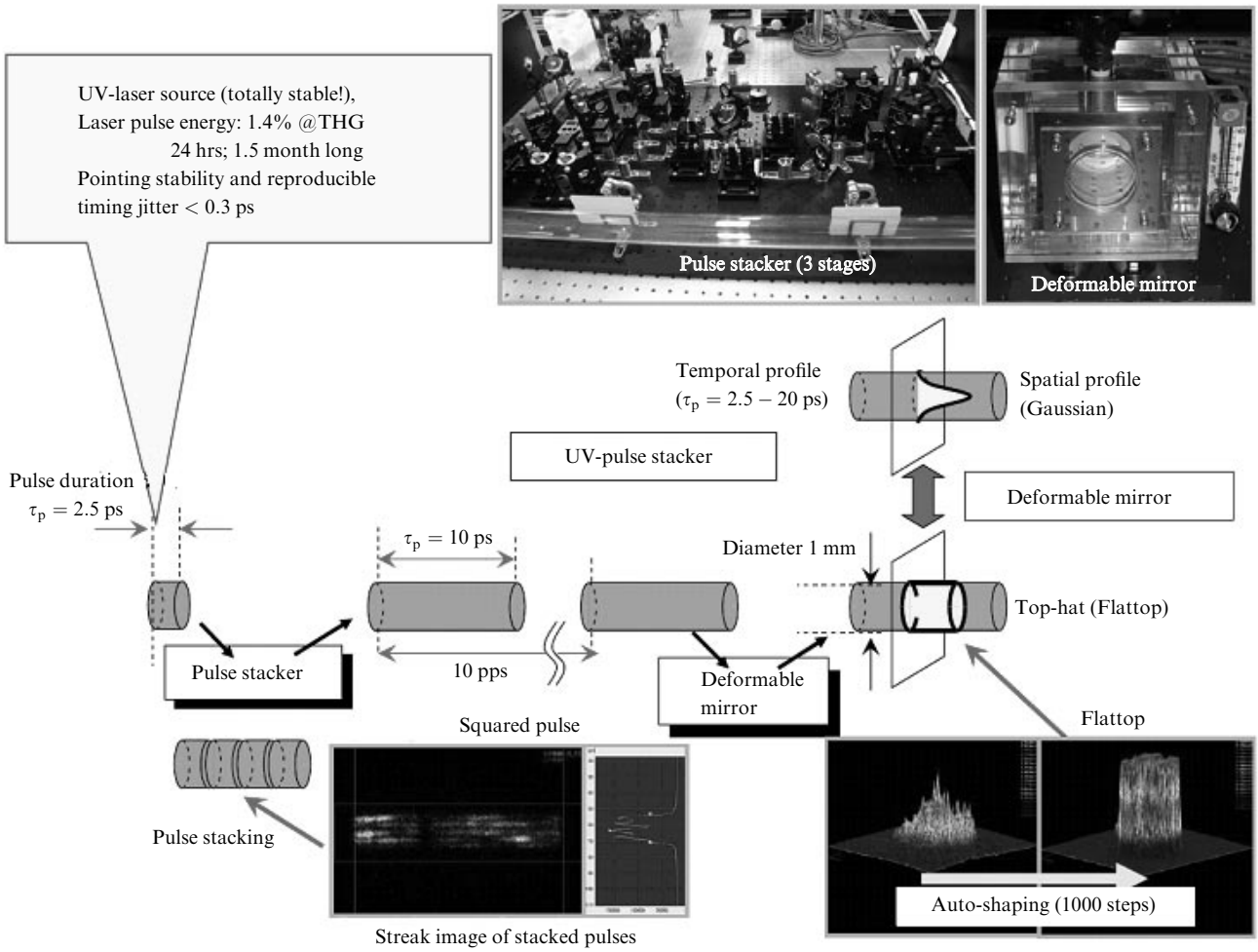

Figure 3. Three-dimensionally [spatially (2D) and temporally (1D)] UV-laser pulse shaping system. The 3D shaping system consists of a deformable mirror (DM) and a pulse stacker. These two shaping techniques can be optimised independently, since there is no interference between them. The schematic drawing of pulse stacking shows 10-ps pulse generation by stacking four 2.5-ps micro pulses (two stages of pulse stackers).

voltages is between 0 and 250 V in steps of 1 V, making it possible to shape arbitrary spatial profiles in a total of 250^{59} ($\sim 10^{141}$) forming possibilities. However, such high adjustability makes manual as well as simple algorithm adjustment impossible.

3.1.1. Experiment on closed loop system for spatial shaping

A closed loop system is essential for a deformable mirror to optimise the laser's spatial profile automatically (Fig. 4). We use a PC to control the electrode voltage of the deformable mirror and to measure the spatial profile with a laser profile monitor (Spiricon, Inc.: LBA300-PC). Laser light is reflected with deformation by the deformable mirror and monitored with the profile monitor, whose analysing program can provide many parameters to evaluate the characteristics of beam profiles. The program is remotely controlled by Active-X [9] control (Object Linking and Embedding), so we could control the deformable mirror while monitoring the laser beam parameters.

3.1.2 Algorithm for automatic control

This spatial shaping method with adaptive optics needs a sophisticated algorithm. We developed software based on a genetic algorithm (GA) to automatically optimise the deformation of the deformable mirror (DM). The set of voltages of whole DM-electrodes are treated as chromosomes in their application. At first, we prepared 50 numbers of chromosomes as the initial population and used the MGG (Minimal Generation Gap) method to select the surviving chromosomes. The 59 DM-electrode voltages are applied independently in the range of 0 to 250 V, and they were coded to 59 elements in a chromosome. In this type of the deformable mirror (electrostatic actuator), the displacement in the central region of the membrane is proportional to the square of electrode voltage. In the initial population, applied electrode voltages (chromosome element values) were randomly selected from the set of discreet voltages (0, 42, 70, 93, 113, 131, 147, 162, 176, 189, 201, 213, 225, 236, 250 V) to linearly change the displacement. In this procedure, chromosomes are treated as follows.

(i) Make a Family consisting of four chromosomes. Two chromosomes are selected randomly from the initial population to make the family, and these chromosomes are placed as 'Parents'. Then, the other two chromosomes as 'Children' are generated through the crossover of the chromosomes of the 'Parents'. In our program, we prepared three different ways of crossover: random crossover (in our case '58-point crossover'), one-point crossover, and two-point crossover. Thus, four chromosomes are prepared and treated as 'Family', which is called 'Generation' in GA.

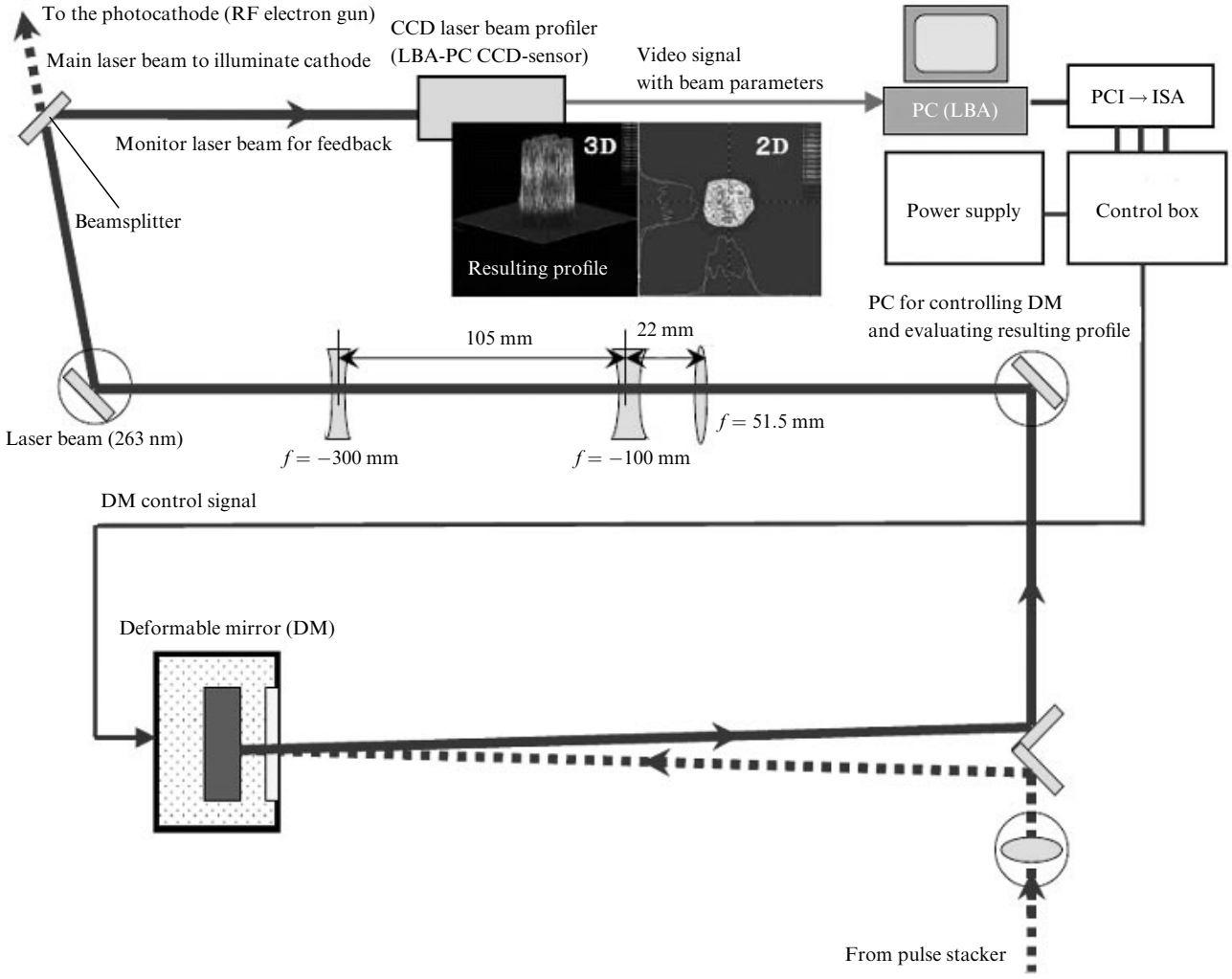

Figure 4. Closed control system for the experiment. With evaluation of top-hat (flattop) profiles on laser profiler (LBA300-PC), the deformable mirror (DM) is automatically controlled to optimise the spatial profile toward the top-hat as a target profile.

(ii) Drive the deformable mirror and obtain results of the laser parameters from measurements of the laser's spatial profile. In the MGG method, the four chosen chromosomes in the family are compared, and the two best chromosomes survive as superior. Drive the deformable mirror by setting the chromosomes of four members of the 'Family' (in the order 'Father', 'Mother', two 'Children') and obtain each result of beam parameters calculated from the analysis program of the laser profile monitor. The beam parameters of the laser's spatial profile are obtained for evaluation in the following step.

(iii) Evaluate the resulting parameters using a fittness function. These results are scored by a fittness function defined by top-hat beam shaping. The fittness function is a linear combination of the nine parameters shown in Table 1 with each coefficient as weight. If a chromosome is more highly scored in the evaluation of the fittness function for top-hat, it will be promoted to a higher position in the ranking of 'Family'. Thus, in this ranking, the chromosomes are ordered by comparing values of the fittness function.

(iv) The best two chromosomes are selected as superior and then returned to the population. This procedure makes one generation step forward, and the population is renewed to initiate the next generation.

3.1.3 Fittness function to optimise spatial profile through evaluation of beam parameters

We chose nine useful parameters [6] to evaluate the top-hat profiles (Table 1.). These parameters for top-hat shaping and their functions are shown in Table 1. A fittness function is made of the linear combination of these parameters. The fittness function is used as an index for the sophisticated program-based genetic algorithm. The more the laser profile is close to the target profile (top-hat), the higher the value of the fittness function is. This is calculated for the spatial profile corresponding to each chromosome to evaluate the spatial profile, spot-size diameter, and center position of the profile. Maximising the value of the fittness function with the GA-program, the computer-aided deformable mirror optimises the profile toward a target spatial profile such as the top-hat. The most representative parameter is the Top Hat Factor (THF) [10], where THF is defined as an integral function of energy fraction as shown in Fig. 5. After 2500 generation steps, an inhomogeneous spatial profile was improved to the quasi-top-hat profile shown in Fig. 6.

Table 1. Parameters and their uses in the fittness function to evaluate spatial profile optimisation.

Parameters of fittness function for Top-hat (flattop) shaping with a deformable mirror	
Beam centre	Minimise the difference from the initial centre position (x, y)
THF [10]	Maximise the Top Hat Factor (0 – 1) (Top-hat: THF = 1.0; Gaussian: THF = 0.5)
Effective area	Maximise the integrated energy within the set circle area
Effective diameter	Minimise the difference from the diameter of set circle
Flatness	Minimise the standard deviation divided by the average top-hat area
Peak-to-peak	Minimise the difference between the maximum and minimum values in a top-hat area
Beam diameter	Minimise the difference from the set diameter
Hot spot (maximum)	Minimise the maximum in a top-hat area
Dark spot (minimum)	Maximise the minimum in a top-hat area

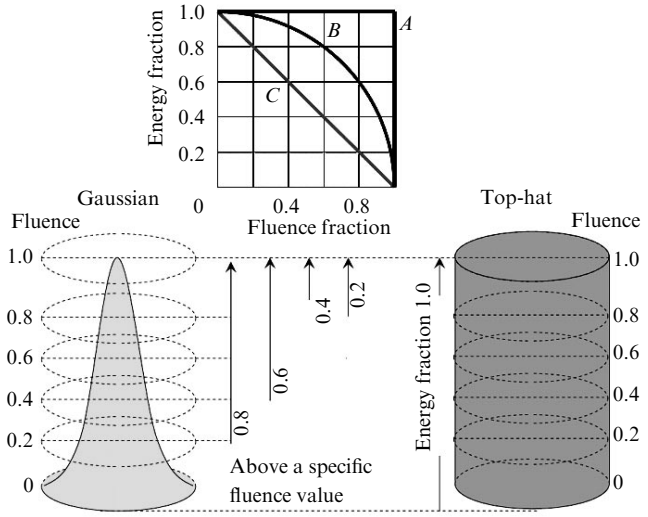

Figure 5. Top Hat Factor (THF) [10] for evaluation of top-hat profiles: In the top figure, curve (A) is a top-hat beam with THF of 1.0, curve (C) is a Gaussian beam, and curve (B) is beam profile between top-hat and Gaussian.

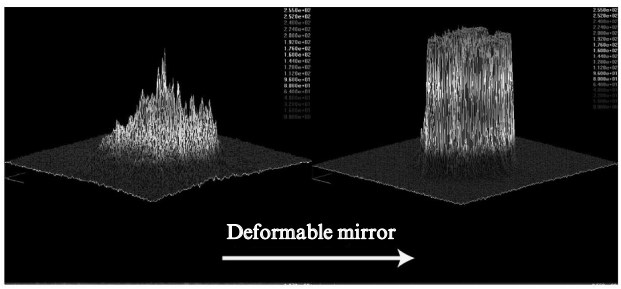

Figure 6. Result of spatial profile optimisation to top-hat with a deformable mirror (laser profile monitor: LBA300-PC).

3.2 Square temporal profile generation with UV-pulse stacker

3.2.1 Principle and configuration of pulse stacker that is not affected by interference

A pulse stacker is composed of sets of half-wave plates and polarising beam splitter cubes. One stage of the pulse stacker consists of a pair of a splitter and a half-wave plate. The full s-polarisation is rotated to 45° with a half-wave plate. It is then divided into an s-polarised pulse and a p-polarised one with the first polarising beamsplitter at each stage. The p-polarised pulse is delayed with an optical delay line and then combined with the s-polarised pulse after using the next polarising beamsplitter at each stage. Finally, as shown in Fig. 7, the laser pulse of 2.5 ps is stacked with optical delay at each stage to generate a longer square pulse. By stacking eight micro pulses in three stages, we can obtain a 20-ps square combined pulse. The polarising beamsplitter cubes used in the first and second stages are of the optical contact type (Showa Optronics Co., Ltd.), considering the high power density of the UV-laser pulse. The polarising beamsplitter used in the third stage is bonded with optical cement because the power density is lower at this stage. The diagram of the optical system and timing chart of the pulse stacker with a three-stage configuration are shown in Fig. 8. At every stage of this pulse stacker, the s-polarisation pulse at the first splitter is always the origin of the optical timing delay (see timing chart of Fig. 8). This makes it possible to keep the same origin of any timing delay, even if a 5-, 10- or 20-ps squarely combined pulse is generated by masking a p-polarisation pulse at each corresponding stage.

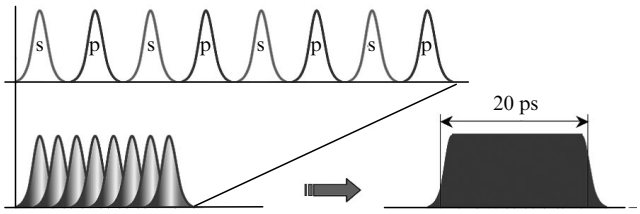

Figure 7. Principle of chirped-pulse stacking (8 pulses: three stages). Avoiding interference, the s- and p-polarised micro pulses are alternatively stacked with the optical delay as long as the micro pulse duration.

3.2.2 Finding the origins of optical delay lines

To generate a long pulse without any timing gap or overlap, the origins of the optical delay lines must be determined with a precision of less than 1 ps. The origin is defined here as the micrometer-level position in the delay line such that the s- and p-polarised pulses reach the cathode at the same time. The procedure determines the origin by using the electron beam pulse generated at the photocathode as follows [8]. The energy of the electron pulse is measured for two laser pulses divided by each stage of the pulse stacker. The energy of the electron beam is measured as beam positions on a florescence profile monitor after a bending magnet downstream of the RF-gun cavity. To eliminate the positioning jitter and short time drift, the beam positions are measured 5000 times. The micrometer position of the p-polarised pulse is tuned as these two electron beam pulses

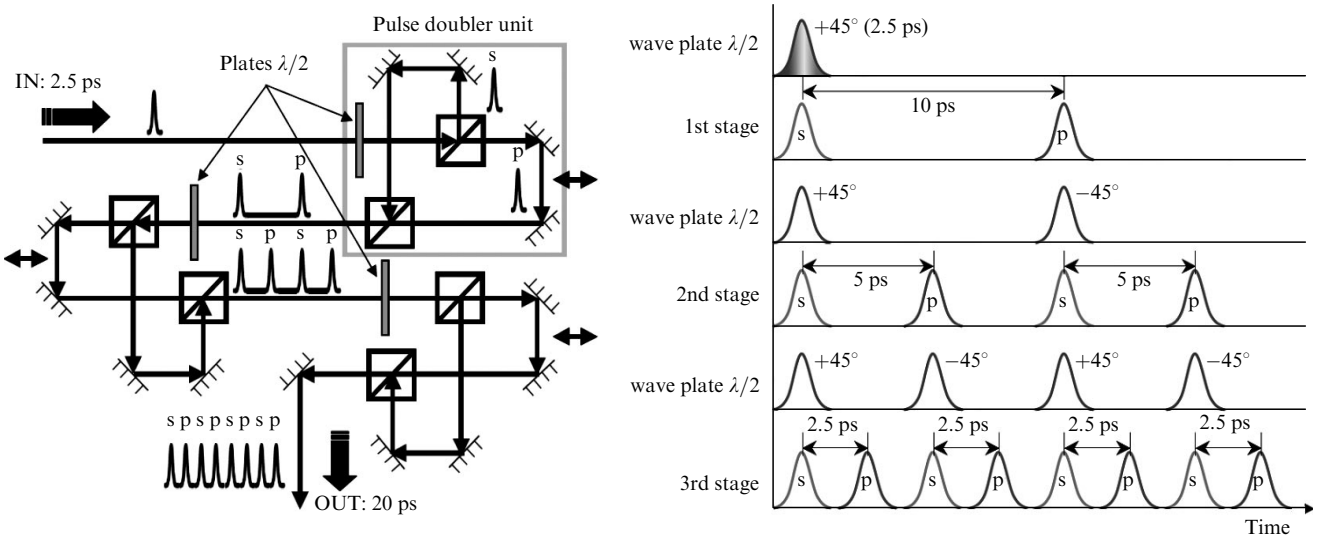

Figure 8. Optical system (left) and timing chart (right) of UV-laser pulse stacker. The drawings are shown in the case of three stages (pairs of polarising UV-laser beamsplitter cubes) of pulse stacker. The initial UV-laser pulse duration is set to 2.5 ps for generating a $\sim$ 20-ps combined macro pulse. The optical kit of this pulse stacker is commercially available from Luminex Trading, Inc. (http://www.luminex.co.jp/) under license of SPring8/JASRI.

come to the same position on the profile monitor after several iterations. The timing precision of the origin was about 0.5 ps, estimated from the position jitter distribution.

4. Conclusions and future developments

Through optimisation with computer-aided DM, we could improve the laser radiation spatial profile. In particular, top-hat shaping was successful in a short time by applying a new program based on a genetic algorithm. At present, there seems to be no difficulty in generating top-hat or homogeneous profiles. However, recently another candidate of a reliable 3D-pulse shape was proposed for even lower emittance [11, 12], which is an ellipsoidal with equivalent fluence along the temporal axis. In this case, a microlens array or deformable mirror cannot help to generate such a three-dimensionally ellipsoidal distribution. In reference [11], a kind of pulse stacker operated by controlling the longitudinal fluence was proposed as a solution to generating an ellipsoidal beam pulse; however, adjustment by this means is not simple. A method using a fibre bundle is one solution to avoid the difficulty of adjusting different optical paths [13]. The fibre bundle is a practical system to shape both spatial and temporal profiles at the same time during laser-pulse transportation. The principle of this shaping method involves, in practice, thousands of pulse stackings in defusing the 3D volume. However, this method has a major disadvantage: it is difficult to make a smaller laser spot size of $\sim$ 1 mm on the cathode for a realistic working distance of $\sim$ 1 m in conventional cathode illumination. Therefore, we proposed this shaping technique for only a backward cathode illumination system to shorten the working distance. For this configuration of backward illumination, we are developing a transparent cathode. We demonstrated spatial and temporal shaping through the fibre bundle with a diameter of 8 mm using a collection of 1300 small fibre strands with a fused end (Fig. 9). The results of this shaping experiment are shown in Fig. 10.

Considering the response time of semiconductor photocathodes and the reliability of adjusting the optics, we do

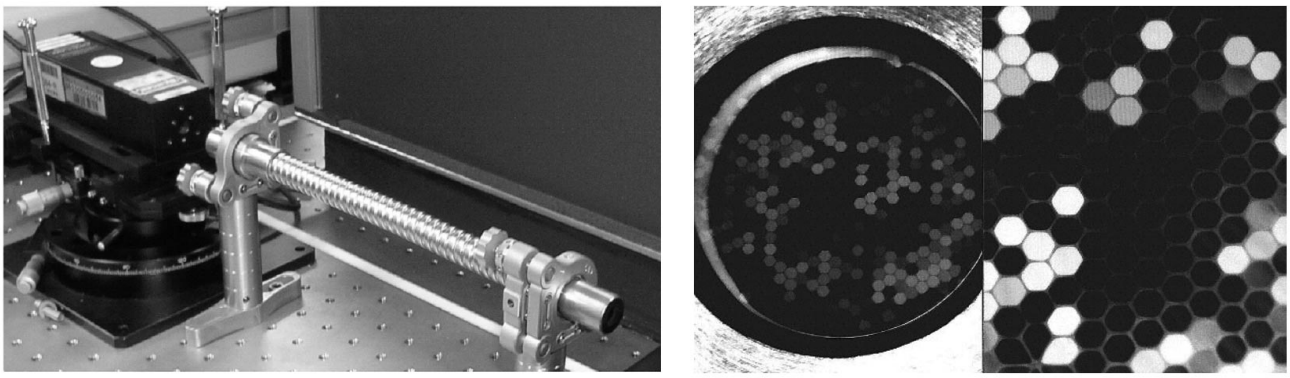

Figure 9. Fused surface structure of a fibre bundle (diameter of 8 mm; collection of 1300 small fibre strands). In developing a compact source system for high-quantum-efficiency photocathode backward illumination, the combination of a blue (404 nm) laser diode and the fibre-bundle-based 3D-pulse shaper has been examined (left photo).

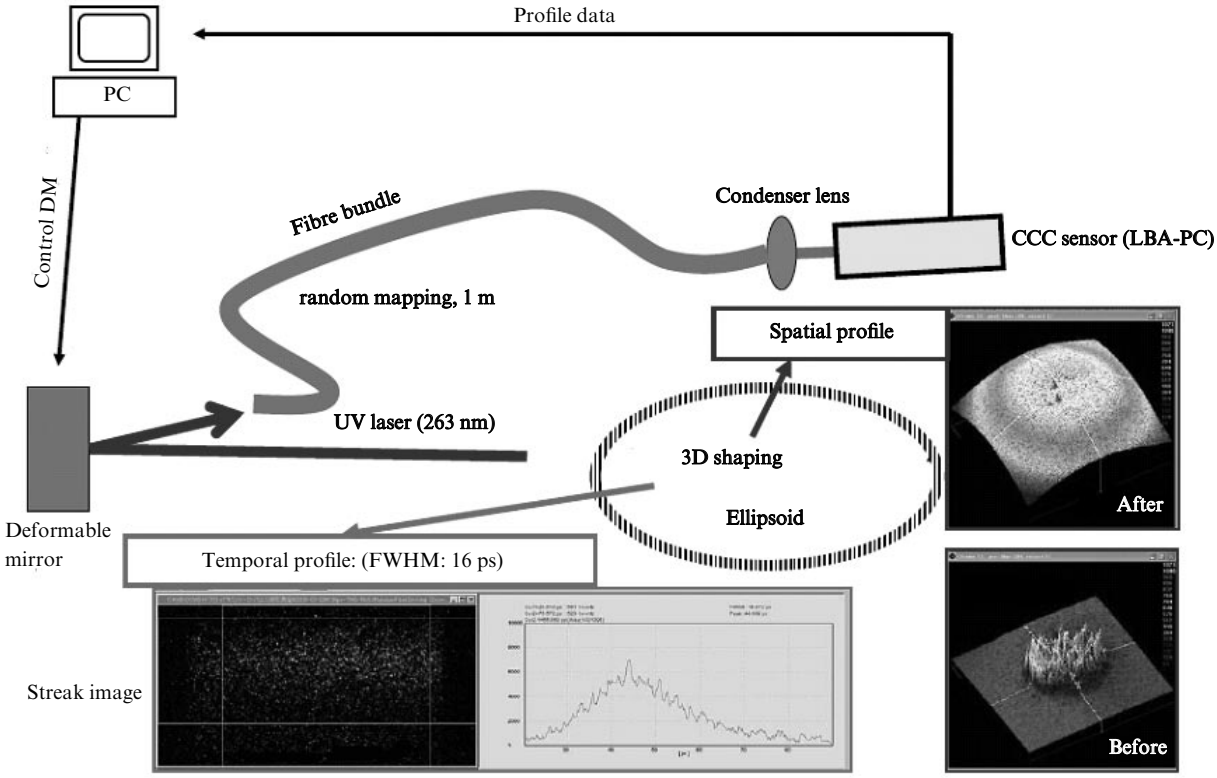

Figure 10. Closed control system for a fibre bundle with a computer-aided DM. The laser spatial profile is homogenised perfectly. At the same time, the temporal profile is elliptically shaped. The shaping results shown for both the spatial and temporal profiles were done by using only the fibre-bundle shaper. Without using DM and GA, it is possible to generate a 3D quasi-ellipsoidal pulse. By applying a computer-aided DM as shown in this figure, the 3D pulse shape can be precisely optimised.

not yet have a reliable solution for generating this reliable ellipsoidal electron pulse from a photocathode. However, we plan to apply adaptive optics such as a deformable mirror to automatically optimise the electron beam pulse for even lower emittance with a feedback routine. To accurately shape an ellipsoidal profile, it is possible to combine the fibre bundle with a deformable mirror to control the spatial distributions of the incident laser. Automatic optimisation with a deformable mirror can be a powerful tool for optimising 3D electron beam pulse shapes with a genetic algorithm, if the most probable solution is within its search range (Fig. 10).

For the shot-by-shot optimisation of each laser-pulse profile, the laser system should be passively stabilised through environmental controls. At present, the long-term (continuous operation for 1.5 months) pulse-energy stability of THG has been improved to less than 1.4 %, which is a sufficient laser source for shot-by-shot automatic optimisation with adaptive optics. At the present status of the laser oscillator under environmental controls, its mode-locking has remained continuously stable with a locked repetition rate of 89.25 MHz for five months. Furthermore, continuous operating time of the YAG laser due to the lifetime of the flash lamp, which is now limited to around five months (in our record, 119, 380, 846 shots at max.) while maintaining such high stability of laser's pulse energy. Continuous operation with gradually arising flash lamp voltage increases the lifetime of the flash lamp five times without losing stability of the laser's pulse energy. If the oscillator is stable without out-of-mode locking, the overall laser system can remain stable for yearlong operation with the energy stability described above. During this potentially continuous yearlong operation, every laser parameter was kept constant without any signs of instability.

We demonstrate 3D shaping [both temporal (1D) and spatial (2D)] short pulse (5–20 ps) laser beam as an ideal light source for yearlong stable generation of a low emittance electron beam with a high charge. At present, we apply a deformable mirror that automatically shapes the spatial UV-laser profile with a feedback routine, based on a genetic algorithm, and a pulse stacker for temporal shaping at the same time. The 3D shape of the laser pulse is spatially top-hat (flattop) and temporally – a square stacked pulse. Using a 3D-shaped laser pulse with a diameter of 0.8 mm on the cathode and pulse duration of 10 ps (FWHM), we obtain a minimum horizontal normalised emittance of 1.4π mm mrad with beam energy of 26 MeV, holding its net charge to 0.4 nC pulse^{-1}. At a higher net charge of 1.0 nC pulse^{-1}, the minimum beam emittance is 2.3π mm mrad with an equivalent diameter and a longer pulse duration of 20-ps (FWHM). This high-brightness electron source has maintained almost enough low emittance for X-ray FEL requirements during yearlong continuous operation. Precisely optimising 3D-shape of laser pulse, we are challenging to generate high brightness beam with an emittance as low as possible.

To achieve adaptive control of the temporal parameters of the laser pulses, we are preparing a programmable pulse shaping system in the fundamental wavelength region by using a spatial light modulator (SLM) based on fused-silica

plates (Cyber Laser Inc.) [14]. The temporal profile is measured with a streak camera or FROG (Frequency-Resolved Optical Gating). We implemented an adaptive optical pulse-shaping system using both the deformable mirror (DM) and the SLM at the end section of laser system. We are developing a sophisticated program to examine both the spatial and temporal shaping abilities of original inhomogeneous UV-laser profiles. In the future, we plan to apply this adaptive optical complex (DM & SLM) to directly optimise the 3D shape of the electron beam pulse generated from a photocathode for further extreme low emittance with a feedback routine. With this procedure, we expect more reliable electron beam profiles to be generated with compensation for some of the optical distortions and the inhomogeneous distribution of the quantum efficiency on the cathode surface. However, it is important to clarify the phenomena related to laser incidence on the cathode, and we will thoroughly investigate this together with cathode surface physics.

Acknowledgements. Many companies have contributed toward the development and understanding of long-term stability problems in our laser system and reliable pulse shaping of THG. The authors wish to thank the entire staff at Femtolasers Produktions GmbH, H. Jousselin (THALES LASER Co., ltd.), and K. Takasago (Cyber-Laser Inc.). Part of this work on developing the spatial light modulator (SLM) based on fused-silica plates was supported by the Advanced Compact Accelerator Development Project in Japan.

References

1. Taniuchi T. et al. *Proc. 18th. Int. Free Electron Laser Conf.* (Rome, Italy, 1996) p. 137 – 139.
2. *Linac Coherent Light Source (LCLS) Conceptual Design Report,* SLAC-R-593, April 2002.
3. *TESLA Techn. Design Report, Pt V, The X-Ray Free Electron Laser* (March 2001). Ed. by G. Materlik and Th. Tschentscher.
4. Rivers J. *SCSS X-FEL Conceptual Design Report, RIKEN*, May 2005.
5. Tomizawa H. et al. *Proc. EPAC' 2002* (Paris, 2002) pp 1819 – 1821.
6. Tomizawa H. et al. *Proc. 27th. Int. Free Electron Laser Conf.* (Stanford, US, 2005) pp 138 – 141.
7. Yang J. et al. *J. Appl. Phys.*, **92**, 1608 (2003).
8. Dewa H. et al. *Proc. 28th. Int. Free Electron Laser Conf.* (Berlin, Germany, 2006) (in press).
9. Operator's Manual, Model LBA PC Series, Version 2.50, Spiricon Inc.: Ch. 9 ıActiveXı.
10. Operator's Manual, Model LBA PC Series, Version 2.50, Spiricon Inc.: Ch. 6.19 'Top Hat Factor'.
11. Limborg-Deprey C., Bolton P.R. *Nucl. Instrum. Meth. Phys. Res. A*, **557**, 106 (2006).
12. Limborg-Deprey C., Tomizawa H. *Proc. Phys. Appl. High Brightness Electron Beams* (Erice, Italy, 2005) (in press).
13. Tomizawa H. et al. *Nucl. Instrum. Meth. Phys. Res. A*, **557**, 117 (2006).
14. Tomizawa H. et al. *Proc. LINAC' 2004* (Luebeck, Germany, 2004) pp 207 – 209.